Research article

Neural activation patterns and connectivity in visual attention during number and non-number processing: An ERP study using Ishihara pseudoisochromatic plates

Faraj Al-Marri[1,2], Faruque Reza[1,*], Tahamina Begum[1], Wan Hazabbah Wan Hitam[3], Goh Khean Jin[4], Jing Xiang[5]

[1] *Department of Neuroscience, School of Medical Sciences, Universiti Sains Malaysia, 16150 Kubang Kerian, Kota Bharu, Kelantan, Malaysia*
[2] *Department of Neuroscience, College of Medicine, King Faisal University, 31982 Hofuf, Al-Ahsa, Saudi Arabia*
[3] *Department of Ophthalmology, School of Medical Sciences, Universiti Sains Malaysia, 16150 Kubang Kerian, Kota Bharu, Kelantan, Malaysia*
[4] *Division of Neurology, Faculty Of Medicine, Universiti Malaya, 50603 Kuala Lumpur, Malaysia*
[5] *Division of Neurology, MEG Center, Cincinnati Children's Hospital Medical Center, 3333 Burnet Avenue, Cincinnati, OH 45220, USA*

*Correspondence: faruque@usm.my, faruquereza@gmail.com (Faruque Reza)

https://doi.org/10.31083/JIN-170058

Abstract

Visual cognitive function is important in the construction of executive function in daily life. Perception of visual number form (e.g. Arabic digits) and numerosity (numeric magnitude) is of interest to cognitive neuroscientists. Neural correlates and the functional measurement of number representations are complex events when their semantic categories are assimilated together with concepts of shape and color. Color perception can be processed further to modulate visual cognition. The Ishihara pseudoisochromatic plates are one of the best and most common screening tools for basic red-green color vision testing. However, there has been little study of visual cognitive function assessment using such pseudoisochromatic plates. 25 healthy normal trichromat volunteers were recruited and studied using a 128-sensor net to record event-related electroencephalogram. Subjects were asked to respond by pressing numbered buttons when they saw the number and non-number plates of the Ishihara color vision test. Amplitudes and latencies of N100 and P300 event related potential components were analyzed from 19 electrode sites in the international 10–20 system. A brain topographic map, cortical activation patterns, and Granger causation (effective connectivity) were analyzed from 128 electrode sites. No significant differences between N100 event related potential components for either stimulus indicates early selective attention processing was similar for number and non-number plate stimuli, but non-number plate stimuli evoked significantly higher amplitudes, longer latencies of the P300 event related potential component with a slower reaction time compared to number plate stimuli imply the allocation of attentional load was more in non-number plate processing. A different pattern of the asymmetric scalp voltage map was noticed for P300 components with a higher intensity in the left hemisphere for number plate tasks and higher intensity in the right hemisphere for non-number plate tasks. Asymmetric cortical activation and connectivity patterns revealed that number recognition occurred in the occipital and left frontal areas where as the consequence was limited to the occipital area during the non-number plate processing. Finally, results demonstrated that the visual recognition of numbers dissociates from the recognition of non-numbers at the level of defined neural networks. Number recognition was not only a process of visual perception and attention, but was also related to a higher level of cognitive function, that of language.

Keywords

Visual number recognition; event related potential; pseudoisochromatic plates; N100 and P300 event; attention; effective connectivity

Submitted: August 22, 2017; **Accepted:** October 17, 2017

1. Introduction

The brain and eye analyze the visual perception of brightness, movement, shape, and color of objects [1, 2] even the mental imagery of motion and static visual features [3, 4]. The three basic color receptors of blue, green, and red have their own photo pigments that react to light to evoke receptor potentials in the visual pathway. The Ishihara test is one type of test where a chart can be employed to detect weak or missing L-cones (red) and M-cones (green), but not S-cones (blue) [5, 6]. Different colored plates are used in this test, where primary and secondary dots form number or non-number shapes. Secondary dots play a role in the background of the plates [7]. Subjects are classified as having impaired color vision if two or more plates are recognized incorrectly [8]. Impaired color vision influences visual cognitive functions involved in object recognition, color memory, color consistency, and discounting of the illuminant [9, 10]. However, visual information processing can be divided into two general pathways: a neural pathway for vision from retina to cortex and a multi-synaptic corticocortical pathway for visual streams. The former consist of the retina, optic nerve, optic

 ©2018 The authors. Published by IMR press. All rights reserved.

chiasm, optic tract, lateral geniculate body (LGN) of the thalamus, geniculocalcarine tract or optic radiations, and primary visual cortex (V1, also known as Brodmann's area 17). These anatomical visual pathways are of great interest to ophthalmologists and neurologists following injury or impairment of vision. The latter consist of the so-called 'ventral stream' (also called the what pathway) and 'dorsal stream' (also called the where pathway) [11, 12], which have attracted much attention from cognitive neuroscientists. The ventral stream originates from V1 of the occipital lobe and spreads along the ventral surface of the temporal lobe (occipitotemporal). It is involved in the processing of the recognition of objects, forms, face, color, and numerals. Conversely, the dorsal stream also originates from V1 and spreads along the dorsal surface of the parietal lobe (occipitoparietal). It is involved in the processing of the spatial location of objects. Likewise, numerical information from a visual scene is encoded and processed along the occipitoparietal (dorsal stream) pathway and finally projected to number-selective circuits of the bilateral intraparietal sulcus [13]. Such hemispheric activation or lateralization, identified by the triple code model (TCM), also originates not only from number processing but also from arithmetical skill processing which has been assessed recently in adults by functional transcranial doppler ultrasonography [14]. The TCM of number processing is a theoretical framework proposed to be organized through three circuits – a linguistically mediated verbal coding circuit associated with the left hemisphere, a visual number coding circuit for recognition of Arabic digits associated with the bilateral fusiform and lingual regions of the ventral stream of object recognition, and a bilateral number magnitude (cardinal value/numerosity) coding circuit [15].

Alternatively, cognitive function, can be simply described as the mental process that takes internal or external input and transforms, minimizes, elaborates, stores, retrieves, and finally utilizes it [16]. The term cognition covers a variety of functions such as attention, memory, learning, calculating, problem-solving, decision-making, reasoning, and planning [17–19]. Among all those sub-components of cognitive function, attention has a large role in regulating cognitive function [20]. The brain areas activated by visual stimuli have been investigated by different neuroimaging modalities such as MEG, fMRI, and PET, among others. A recent review article [21] of a functional neuroimaging meta-analysis highlighted that a number form area, proposed to be specialized for Arabic numerical processing, is in the right inferior temporal gyrus, bilateral parietal, and superior and inferior right frontal regions. Event-related potential (ERP) studies provide another method to measure visual cognitive function (attention) at the electrophysiological level. Due to higher temporal resolution, the electroencephalogram (EEG)/ERP has great importance in cognitive neuroscience research, as has fMRI, which has better spatial resolution. Moreover, using electrophysiological techniques, the connectivity of the brain has recently received increased attention, which has supported the development of brain cognition and action that can determine a temporal correlation [22].

In this study, a stimulus is being employed that has the capacity to simultaneously activate the processing of colored numbers and non-numbers in the brain to enable determination of how the brain processes activation, connectivity, integration, or segregation of different visual features in the visual system. Such a stimulus could provide an important test tool for understanding certain brain disorders, such as attention deficit disorder, and connectivity disorders in different sensory areas of the brain. Several investigators consider that connectivity can be reformed for various reasons in mental tasks [23], by sleep [24], by learning [25], and by consciousness [26]. Lower connectivity has been identified in the fronto-parietal network among subjects with reading difficulty [27, 28] and this network is vital for visual attention during reading [29]. There is also evidence that enhanced connectivity within visual processing components is further increased between visual processing and temporal-occipital components [30]. Moreover, left temporal-parietal connectivity is stronger during the processing of arithmetic principles and language than during computation, whereas parietal-occipital connectivities are stronger during computation than during the processing of arithmetic principles and language [31]. One example of connectivity disorders in different sensory areas of the brain is synesthesia, a neurological phenomenon in which an individual perceives a specific color when seeing a specific number [32]. Synesthesia can also occur when a letter is interpreted as a color and a taste for a shape. Grapheme synesthesia occurs when a color is experienced upon seeing letters and numbers. It is a phenomenon arising from cross connectivity between a color area and a number area in the fusiform gyrus. Research has verified that Arabic numerals but not Roman numerals induce color. This is interpreted as demonstrating that the visual image, or "grapheme" of a number that is predominant, rather than the numerical concept [33, 34]. Ramachandran and Hubbard [33] have also shown that synesthetic subjects are significantly better at identifying an embedded shape than Non-synesthetes, which is comparable to the way control subjects see colored patterns in the Ishihara color-vision test. Moreover, attention plays a vital role in modulating synesthesia, as during attention-demanding tasks colour often weakens synesthetic experience [35].

Visual attention is a one of the primary steps in the construction of executive function. Reaction or response time (RT) can be measured to examine visual attention [36, 37]. RT quantifies the temporal gap between the start of a stimulus and a subject's response. RT can be used as a measure of awareness in the activities of daily life. Gender, age, level of fatigue, and health influence RT [38]. There are three types of RT: simple, recognition, and choice, with one response, no response, and multiple responses, respectively [39, 40]. Choice RT is more important than the other RTs in everyday life. Visual or auditory inputs are important in the measurement of visual or auditory choice RTs. Due to different sensitivities to the wavelength of red, green, and blue light, RTs are faster or slower [41]. Visual choice RT is faster in males than females and in hand dominant subjects [42]. Faster RT emphasizes a faster processing time by the nervous system and faster muscular movement [43], which is defined as a higher cognitive function [44]. Interestingly, a recent study investigated the 'mental number line' which is oriented from left to right on the SNARC (spatial-numerical association of response codes) effect (faster response to the small number on the left side and to the large numbers on the right side) using kinematics of fingers movement besides response time and found that numerical processing affects action execution [45]. Therefore, RT was used as a marker of cognitive processing speed in this study, together with ERPs. There are several components of ERP waveforms depending on the particular stimulus. ERP waveforms can be evoked during visual stimuli. The N100 or N1 ERP component is the negative deflection evoked approximately 100 ms after a stimulus [46, 47]. N100 is the sensory component that indicates selective attention and voluntary discrimination processes [48, 49] a priming stimulus is matched [50]. Alternatively, P300 or P3 is the positive ERP component evoked approximately 300 ms after a stimulus [51, 52]. P300 is a cognitive component,

where a higher amplitude indicates higher cognitive involvement, which in turn is taken to mean greater attention [53].

Color and texture are processed in medial temporal-occipital areas and geometric features are processed in lateral temporal-occipital areas [54]. Though some studies have employed simple color stimuli [54, 55], there is a near complete absence of visual cognitive function assessment using pseudoisochromatic plates. For this reason, visual numerical cognitive function was investigated here using the Ishihara test and the ERP indexing procedure, and RT and EC effective connectivity analysis. Additionally, brain topography was defined to understand hemispheric lateralization associated with the two stimuli.

2. Methodology

2.1. Ethics and sample size

Ethical permission was obtained from the human ethical committee of the Universiti Sains Malaysia (USM) [USM/KK/PPP/JePeM 232.3(8)]. Subjects were recruited via the internet, email notification, and personal communication. All participants gave written informed consent before starting the experiment. A total of 25 (13 male and 12 female) healthy subjects were recruited who had normal or corrected-to-normal vision and no neurological or other major diseases. Sample size was calculated using power and sample size (PS) software (PS version 3.1.2) supported by data from a related study [56]. Inputs for sample size calculation were $\alpha = 0.05$, power = 0.9, $\delta = 3.9$ and $\sigma = 5.8$. The study was performed in the MEG/ERP laboratory of the Hospital Universiti Sains Malaysia (HUSM).

2.2. Study procedure

Each subject sat in a sound-proofed and dimly lit room with a 128-channel geodesic sensor net (GSN) from Electrical Geodesic Inc. (EGI) (Eugene, OR) on their head. Before application, the net head circumference of a subject was measured for calculation of the proper net size, and the net was soaked with an electrolyte solution. After each use, the net was rinsed and disinfected for the next subject. A simple visual oddball paradigm was employed by using 18 Ishihara color vision tests plates, including nine number (transformation and vanishing type) and nine non-number plates. The 18 plates were used three times, and a total of 54 stimuli (27 numbers and 27 non-numbers) were used in one session. E-prime software (v 2.0) was used for stimulus presentation.

2.3. Experimental procedure

Subjects sat 80 cm from a 22″ LCD computer monitor where all stimuli were presented at the centre of the screen for the subject's response. Subjects were asked to press either button '1' or button '2' as quickly and correctly as possible if the stimulus was either a number plate or a non-number plate, respectively. Stimuli were presented for one second with a 0.5 sec fixation and 1.5 sec inter-stimulus interval (Fig. 1).

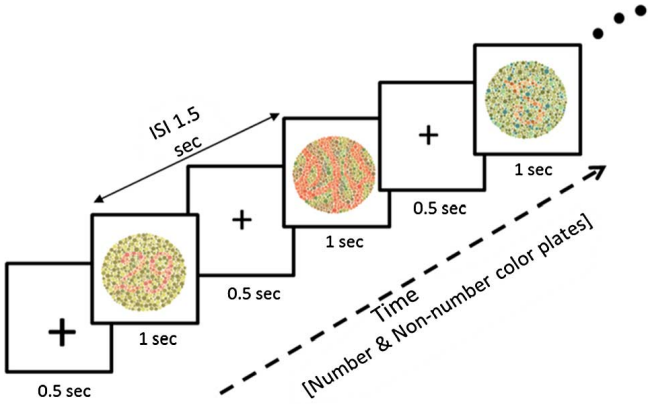

Fig. 1. Graphical representation of experimental procedure with number and non-number plates of the Ishihara color vision test.

2.4. Data recording and analysis

RT recorded for the button press event, and a *t*-test was employed to analyze correct and incorrect responses.

EEG data was recorded with a Net Amps 300 amplifier and Net station software. Sampling rate was 250 Hz, and electrode impedances were below 50 KΩ. Data were filtered with 30 Hz low-pass and 0.3 Hz high-pass filters, segmented 100 ms before and 800 ms after stimulus presentation, and baseline corrected before 100 ms of stimuli. Eye movement, eye blink, and movement artifacts were removed with an artifact removal tool. The amplitude and latency of N100 and P300 ERP components were then computed from 19 electrodes selected from the 128 electrode employed for the 10–20 international electrode placement system. All procedures were conducted with Net station software. After ERP data extraction, data were pre-processed for outliers, with no correction for N100 and P300 latency outliers. One subject exhibited outliers for N100 and P300 amplitudes of number and non-number stimuli and one subject showed outliers in N100 and P300 amplitude for number plate stimuli. Outliers were identified and replaced by an estimation method for series mean using SPSS version 22 statistical software. To determine the significance of amplitude and latency values of N100 and P300 ERP components for the two categories of number and non-number from the 19 EEG electrodes, both distribution-free nonparametric Wilcoxon signed rank tests and parametric paired *T*-tests were used.

For brain topography and cortical source localization from all 128 EEG electrodes, standardized low-resolution brain electromagnetic tomography (sLORETA) was performed with Brainstorm [57], which is documented and freely available for download online under the GNU general public license (http://neuroimage.usc.edu/brainstorm).

Analysis and visualization of effective connectivity (*Granger causality*) over all 128 EEG electrodes employed the MATLAB (MathWorks, Inc)-based connectivity analysis software HERMES [58] (http://hermes.ctb.upm.es).

3. Results

3.1. Reaction time (RT), N100 ERP component, and P300 ERP component

RT was significantly longer for non-number plate stimuli (570.33 ± 158.43 ms) than number plate stimuli (557.03 ± 151.91 ms) (p = 0.045) (Fig. 2).

The N100 ERP component was not significantly increased in response to number plate stimuli at 12 electrode sites (Fp1, Fp2, F4, F8, C4, P3, P4, O1, O2, Fz, Cz, and Pz) compared with the

Table 1. Peak amplitude of N100 ERP component μ V (mean $\pm$ SD)

	Number plate			Non-number plate			Wilcoxon		Paired *T*-test		
Sites	Mean	$\pm$ SD	Variance	Mean	$\pm$ SD	Variance	*Z*-value	*p*-value	*t*	df	*p*-value
Fp1	1.91	2.22	4.91	1.43	1.92	3.70	−1.197b	0.231	1.36	24	0.186
F3	1.47	2.43	5.92	1.66	1.66	2.76	−0.632c	0.527	−0.54	24	0.598
F7	1.18	1.49	2.23	1.32	1.31	1.72	−1.117c	0.264	−0.45	24	0.657
Fp2	2.22	2.30	5.28	1.37	2.05	4.19	−1.897b	0.058	2.33	24	*0.028**
F4	1.94	1.81	3.29	1.51	1.72	2.97	−1.009b	0.313	1.30	24	0.206
F8	1.64	1.14	1.29	1.14	1.25	1.57	−1.628b	0.104	1.82	24	0.082
C3	1.58	1.41	1.98	1.73	1.61	2.60	−0.256c	0.798	−0.61	24	0.550
C4	1.79	1.26	1.58	1.60	1.23	1.53	−0.444b	0.657	0.75	24	0.464
T3	0.99	1.11	1.23	1.57	1.16	1.34	−1.870c	0.061	−1.95	24	0.063
T4	1.72	1.21	1.47	2.02	1.82	3.33	−0.309c	0.757	−0.81	24	0.429
P3	1.77	1.30	1.69	1.60	1.16	1.34	−0.659b	0.510	0.73	24	0.473
T5	2.08	2.19	4.81	2.15	1.47	2.18	−0.498c	0.619	−0.19	24	0.853
P4	2.61	1.07	1.14	2.30	1.36	1.84	−1.251b	0.211	1.05	24	0.306
T6	3.09	1.65	2.71	3.17	2.45	5.99	−0.309b	0.757	−0.18	24	0.855
O1	2.42	2.77	7.66	2.18	2.08	4.34	−1.170b	0.242	0.57	24	0.577
O2	2.88	2.68	7.18	2.62	2.34	5.50	−0.605b	0.545	0.72	24	0.479
Fz	1.68	1.86	3.46	1.63	1.84	3.39	−0.040c	0.968	0.16	24	0.871
Cz	1.90	1.89	3.58	1.89	1.59	2.52	−0.256c	0.798	0.04	24	0.971
Pz	2.02	1.48	2.20	1.82	1.48	2.19	−0.955b	0.339	0.55	24	0.586

b, c based on positive & negative ranks respectively, * significant if $p < 0.050$.

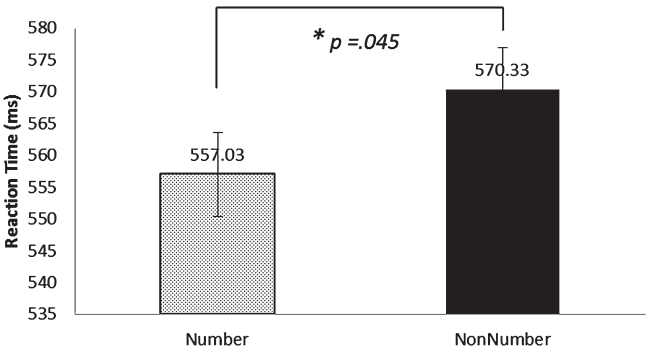

Fig. 2. Mean RT during presentation of number (white dotted column with standard error bars) and non-number (black column with standard error bars) plates of an Ishihara color vision test. RT was significantly increased for non-number plates indicating subjects responded to number plates more rapidly than non-number plates.

non-number stimuli. A significantly higher amplitude was found at the Fp2 electrode position, $p = 0.028$ ($t = 2.33$, df = 24) with a paired *t*-test but there was no significance with the Wilcoxon test (Table 1).

In the case of N100 latencies, a trend for shorter latencies wasobserved at 10 electrode sites (Fp1, F7, Fp2, F4, F8, T3, T4, T6, O2, and Fz) during number plate stimuli when compared to non-number plate stimuli for which only the Fp2 site showed significance for the Wilcoxon test ($p = 0.032$) (Table 2).

The majority of electrode positions (12 of 19 sites: F4, C3, C4, P3, P4, T3, T4, T5, T6, O1, O2, and Cz) showed higher amplitudes of the P300 ERP component during non-number plate stimuli, for which T4 and T6 were highly significant for both non-parametric and parametric tests, when compared to the number plate stimuli, a tendency for higher amplitude was observed in the left frontal hemisphere (Fp1, Fp2, F3 and F7) for number stimuli and for which Fp1 was significant ($t = 2.35$, df = 24) for only the parametric test (Table 3). At about the P300 ERP latency, non-number plates evoked longer latencies at 15 sites (Fp1, F3, F7, F8, C3, T3, P3, P4, T5, T6, O1, O2, Fz, CZ, and Pz). A significantly longer latency was found at the Pz location for both Wilcoxon ($p = 0.036$) and paired *t*-test ($t = -2.07$, df = 24), while the remaining electrode locations showed a tendency towards longer latencies (Table 4).

Grand averaged waveforms from twenty five subjects are shown in Fig. 3 with their N100 and P300 ERP components from 19 electrode channels: Fp1, Fp2, F3, F4, F7, F8, C3, C4, T3, T4, T5, T6, P3, P4, O1, O2, Fz, Cz, and Pz.

3.2. *Brain topography and cortical activation*

A scalp topography map for the N100 ERP components showed similar patterns for both number and non-number plate conditions except for a more intense map at the occipital area for number plates, which was also reflected in the non-significant amplitude increase, as seen in Fig. 4 and Fig.5. However, interestingly, a scalp topography map for the P300 components showed different relationships, such as in the case of the number plates. That was more intense in the left hemisphere, which was opposite the non-number plates which were more intense in the right hemisphere.

Cortical activation patterns during number (Fig. 4) and non-number plate tasks (Fig. 5) in relation to N100 and P300 ERP components are shown in Table 5. Interestingly, in terms of Brodmann's cortical area, the activation pattern of P300 ERP components for the number plate was limited to two Brodmann's regions for each hemisphere, whereas for non-number plates, there were three for each hemisphere; moreover, inter- and intra-hemispheric differences were noticed in the responses to these two stimuli.

3.3. *Connectivity analysis of the evoked response*

Effective connectivity (Granger causality measure), showed a causal effect, interestingly, in the area of the left inferior frontal lobe (near F7) and temporal lobe (near T3), near the mid-parietal (Pz) and

Table 2. Latencies for N100 ERP component (mean ± SD ms)

	Number plate			Non-number plate			Wilcoxon		Paired *T*-test		
Sites	Mean	± SD	Variance	Mean	± SD	Variance	*Z*-value	*p*-value	*t*	df	*p*-value
Fp1	109.44	19.93	397.17	111.84	17.79	316.64	−0.419b	0.675	−0.52	24	0.610
F3	105.44	17.88	319.84	104.8	19.83	393.33	−0.284c	0.776	0.13	24	0.900
F7	112.48	25.75	663.09	120.48	25.07	628.43	−1.22b	0.222	−1.38	24	0.182
Fp2	107.36	22.59	510.24	117.28	22.62	511.63	−2.14b	*0.032**	−1.80	24	0.085
F4	102.88	16.15	260.69	105.92	20.30	412.16	−0.263b	0.792	−0.81	24	0.423
F8	107.84	20.86	435.31	116.8	23.41	548.00	−1.88b	0.060	−1.58	24	0.128
C3	102.88	17.30	299.36	98.4	17.93	321.33	−0.681c	0.496	1.05	24	0.306
C4	103.04	19.71	388.37	99.68	20.33	413.23	−0.163c	0.871	0.68	24	0.506
T3	109.12	25.76	663.36	120	27.54	758.67	−1.77b	0.076	−1.85	24	0.076
T4	110.08	31.18	972.16	115.84	28.55	815.31	−0.987b	0.324	−0.82	24	0.422
P3	103.68	26.86	721.23	100.32	25.84	667.89	−0.618c	0.537	0.47	24	0.641
T5	116.64	30.65	939.57	116.48	32.28	1041.76	−0.443b	0.658	0.03	24	0.980
P4	112.32	30.29	917.23	106.56	28.07	787.84	−1.10c	0.270	1.01	24	0.321
T6	110.4	31.03	962.67	118.72	32.84	1078.29	−1.08b	0.280	−1.14	24	0.267
O1	121.44	27.73	769.17	120.8	28.59	817.33	−0.130b	0.897	0.14	24	0.891
O2	122.08	27.43	752.16	125.76	26.96	726.77	−0.919b	0.358	−0.73	24	0.473
Fz	105.76	18.48	341.44	112.16	19.30	372.64	−1.76b	0.078	−1.41	24	0.172
Cz	105.28	19.76	390.29	103.52	17.75	315.09	−0.192c	0.848	0.66	24	0.515
Pz	115.36	25.89	670.24	116.32	27.30	745.23	−0.114b	0.909	−0.17	24	0.870

b, c based on positive & negative ranks respectively, * significant if $p < 0.050$.

Table 3. Peak amplitude of P300 ERP component μ V (mean ± SD)

	Number plate			Non-number plate			Wilcoxon		Paired *T*-test		
Sites	Mean	± SD	Variance	Mean	± SD	Variance	*Z*-value	*p*-value	*t*	df	*p*-value
Fp1	4.28	3.50	12.27	2.84	3.62	13.10	−0.256b	0.798	2.35	24	*0.027**
F3	3.08	3.18	10.09	2.77	2.35	5.51	−1.709b	0.088	0.49	24	0.632
F7	1.48	2.73	7.47	1.45	2.43	5.92	−0.525c	0.600	0.04	24	0.966
Fp2	4.91	3.80	14.48	4.21	4.01	16.09	−1.144b	0.253	1.38	24	0.179
F4	3.19	1.79	3.19	3.23	1.65	2.73	−0.013b	0.989	−0.11	24	0.913
F8	1.86	2.16	4.68	1.81	1.48	2.18	−0.094c	0.925	0.12	24	0.907
C3	2.97	2.20	4.84	3.28	2.55	6.51	−0.309c	0.757	−0.62	24	0.542
C4	3.85	1.89	3.59	4.20	1.95	3.78	−0.982c	0.326	−0.99	24	0.331
T3	1.99	2.33	5.43	2.43	2.59	6.69	−1.520c	0.128	−0.79	24	0.44
T4	2.25	3.02	9.15	3.76	3.94	15.55	−2.919c	***0.004****	−3.26	24	***0.003****
P3	2.82	2.40	5.77	2.88	1.81	3.28	−0.605c	0.545	−0.15	24	0.879
T5	2.12	1.96	3.84	2.79	2.24	5.04	−1.359c	0.174	−1.38	24	0.179
P4	2.83	1.88	3.55	3.31	2.08	4.34	−1.574c	0.115	−1.68	24	0.105
T6	1.62	2.65	7.03	2.98	3.02	9.11	−2.839c	***0.005****	−2.66	24	***0.014****
O1	1.70	2.76	7.64	1.99	2.65	7.05	−1.063c	0.288	−0.63	24	0.533
O2	1.24	2.50	6.24	1.61	3.01	9.04	−0.632c	0.527	−0.85	24	0.404
Fz	3.35	2.51	6.30	3.06	2.32	5.38	−0.767b	0.443	0.84	24	0.409
Cz	3.99	2.93	8.60	4.41	2.29	5.23	−0.740c	0.459	−0.71	24	0.485
Pz	3.30	2.92	8.51	2.89	2.68	7.17	−0.955b	0.339	0.63	24	0.535

b, c based on positive & negative ranks respectively, * significant if $p < 0.050$, * bold & italic significant at both Wilcoxon & paired *t*-test.

occipital lobe (O2) during number plate tasks (Fig. 6), but the causal effect was almost solely localized in the occipital area near O1 during non-number plate tasks (Fig. 7).

4. Discussion

Visual cognitive function has been investigated using Ishihara color vision test plates, where number and non-number plates were the stimuli. RT, amplitudes, and latencies of N100 and P300 ERP components, brain topography, and Granger causation (effective connectivity) were analyzed. There were no significant differences between the N100 ERP components obtained for either stimulus, but the non-number plate stimuli evoked significantly higher amplitudes and longer latencies for the P300 ERP component compared to number plate stimuli. Similarly, the reaction time was slower for the non-number plate task. Interestingly, a scalp topography map for P300 components showed different patterns of asymmetry, with a higher intensity in the left hemisphere for the number plate task and higher intensity in the right hemisphere for the non-number plate task. Similarly, analysis of effective connectivity revealed a clear and strong interaction between occipital and left frontal cortices during number plate tasks. During number recognition, the direction of

Table 4. Latencies for P300 ERP component (mean ± SD ms)

	Number plate			Non-number plate			Wilcoxon		Paired *T*-test		
Sites	Mean	± SD	Variance	Mean	± SD	Variance	*Z*-value	*p*-value	*t*	df	*p*-value
Fp1	508.8	160.43	25737.33	511.2	162.47	26397.33	−0.568b	0.570	−0.08	24	0.938
F3	488.64	113.02	12772.91	522.24	112.24	12597.44	−1.339b	0.181	−1.60	24	0.124
F7	416.16	131.12	17191.31	433.12	118.80	14114.03	−0.639b	0.523	−0.58	24	0.569
Fp2	516.16	160.41	25729.97	488	155.05	24041.33	−0.834c	0.404	1.01	24	0.325
F4	518.08	121.31	14716.16	511.04	116.47	13564.37	−0.557c	0.577	0.23	24	0.820
F8	504.16	152.21	23168.64	512.64	146.27	21394.24	−0.341b	0.733	−0.27	24	0.789
C3	501.12	132.44	17540.69	528.16	95.16	9055.307	−0.672b	0.502	−0.87	24	0.391
C4	549.12	117.73	13859.36	544.16	93.18	8681.973	−0.757c	0.449	0.22	24	0.829
T3	475.52	132.17	17468.43	483.84	147.53	21764.64	−0.390b	0.697	−0.40	24	0.691
T4	508.16	138.56	19197.97	497.6	125.14	15660	−0.304c	0.761	0.31	24	0.761
P3	468.64	127.63	16290.24	494.72	95.17	9056.96	−0.972b	0.331	−0.93	24	0.363
T5	419.52	101.20	10241.76	438.4	119.78	14346.67	−0.900b	0.368	−0.90	24	0.375
P4	456.64	116.85	13652.91	509.28	124.93	15606.29	−1.272b	0.203	−2.00	24	0.057
T6	404.16	97.98	9599.307	459.36	125.62	15780.91	−1.758b	0.079	−2.04	24	0.053
O1	401.76	119.86	14365.44	418.24	121.41	14740.11	−1.188b	0.235	−0.74	24	0.467
O2	407.52	150.21	22564.43	423.04	134.20	18009.71	−1.413b	0.158	−0.56	24	0.584
Fz	499.84	136.75	18700.64	503.36	130.76	17098.24	−0.061b	0.951	−0.10	24	0.921
Cz	531.84	113.29	12835.31	548.64	89.61	8030.24	−0.486b	0.627	−0.68	24	0.506
Pz	461.12	144.99	21023.36	521.12	122.52	15011.36	−2.100b	***0.036****	−2.07	24	***0.049****

b, *c* based on positive & negative ranks respectively, * significant if $p < 0.050$, * bold & italic significant for both Wilcoxon & paired *t*-test.

Table 5. Cortical activation patterns during number and non-number plate viewing in relation to N100 and P300 ERP components with closer EEG electrode positions (19 electrodes in 10–20 international system)

ERP components	MNI *x*, *y* & *z* coordinates (millimetres)	Brodmann's area (BA), L-left, R-right	Cortical regions	EEG electrode positions
Number				
N100	−54 −57 14	LBA39	Inferior Parietal Lobule − Intraparietal sulcus − Angular gyrus	P3, T5
	−56 −28 14	LBA41	Temporal lobe − Auditory cortex	T3
	17 70 6	RBA10	Prefrontal Cortex	Fp2
P300	−44 −29 14	LBA40	Inferior Parietal Lobule − Supramarginal gyrus	C3, P3
	−47 17 0	LBA45	Inferior Frontal gyrus − Pars Triangularis (Broca's Area)	F7, F3
	50 −49 24	RBA20	Inferior temporal, Fusiform and Parahippocampal gyri	T4, F8
	17 69 2	RBA10	Prefrontal cortex	Fp2
Non-number				
N100	−28 −94 7	LBA18	Occipital lobe − Secondary visual cortex	O1
	−19 −61 5	LBA23	Posterior Singulate Gyrus	Pz
P300	−55 −56 14	LBA39	Inferior parietal lobule − intraparietal sulcus − Angular gyrus	P3, T5
	−56 −30 14	LBA22	Superior Temporal Gyrus (Wernicke's area)	T3
	−10 −76 14	LBA17	Occipital lobe − Primary visual Cortex	O1
	46 −78 14	RBA19	Occipital Lobe (Secondary visual cortex)	O2, T6
	58 −49 14	RBA39	Inferior parietal lobule − intraparietal sulcus − Angular gyrus	P4, T6
	45 −25 14	RBA40	Inferior parietal lobule (Supramarginal gyrus)	C4, P4

coupling was from the visual occipital area towards the language area of semantic coding, but the effect was restricted to the occipital area during the non-number plate task. Non-number plates evoked longer RTs, higher amplitudes, and longer latencies for the P300 ERP component at most electrode sites, of which two were significant when compared with number plate stimuli. Moreover, left/right asymmetry in the areas of cortical activation, interaction, and direction of the effect of attention control during number and non-number tasks were clearly demonstrated in this study.

RTs quantify the time interval between stimulus occurrence and the voluntary response of a subject. Ghuntla *et al.* [59] proposed reaction time is a substantial physiological parameter that contributes information about how quickly a subject can respond to the perception of a stimulus. Faster RTs indicate shorter nervous system processing times associated with faster muscular movement [43] and are an indicator of higher cognitive function [44]. Correspondingly, with this study, reaction time was different during the visual presentation tasks of number and non-number plates. Reaction time was significantly slower for non-number plates than for the number plates. Due to the similarly colored dot shape design of number and non-number plates, numerical error [60] and confusion [61] are obvious with Ishihara testing, even for trichromats; such difficulties added to visual search and identification of a non-number plate, because after encoding a stimulus, subjects need to match the target with

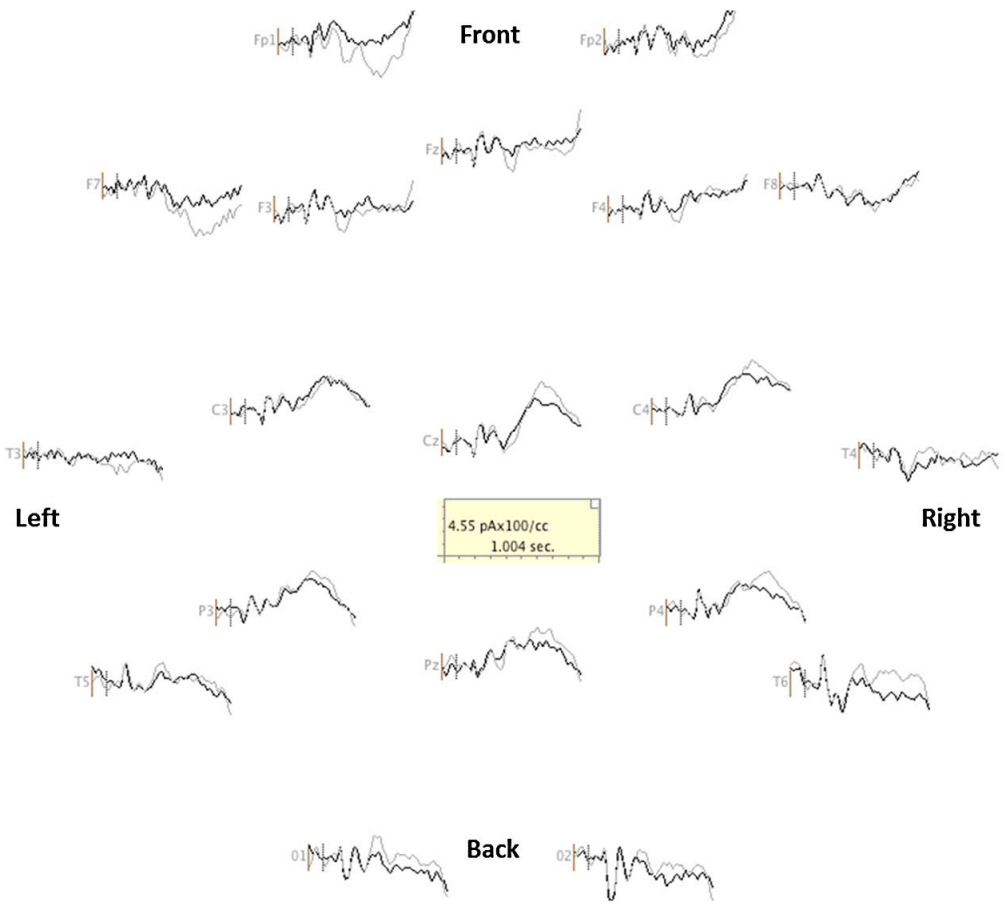

Fig. 3. Arrangement of the grand average waveform of ERP components at 19 scalp sites of electrode channels during the presentation session of number (grey line) and non-number plates (black line), small vertical solid and dotted bars indicate segment time = 0 & stimulation presentation time, respectively. Central rectangle gives scale.

the memorized shape of the correct Arabic digit to achieve accurate responses for non-number pseudoisochromatic plates a decision is made. A significant increase in the mean RT indicated that subjects were taking more time to elicit a convenient intentional response for the relatively complex non-number plates compared with number plates. Luck [62] noted that reaction time is usually affected by the complexity of the stimulus.

The key ERP components for this study were the N100 and P300 ERP. Different colors, shapes or any visual stimuli evokes a N100 ERP component [63] when the subjects are previously experienced with this stimulus [50]. N100 is a marker for visual perception and P300 is an indicator of the higher cognitive functions of attention processing [64]. No significant differences in N100 between number and non-number plates demonstrated that selective attention and a sensory gating mechanism of attention are almost similar for these two stimuli. Regarding the neural sources of N100, based on the result of a scalp topographical map N100 was rather similarly bilaterally distributed for both stimuli, but with a higher intensity for the number plates at occipital (O1 and O2), parietal (P3, P4, and Pz), and frontal (Fp1, Fp2, F4, and F8) locations. Though the differences in this finding were not significant, they were consistent with previous studies [65–67].

The P300 ERP component can be evoked during visual stimulation [68, 69]. Significant differences in P300 between number and non-number plates suggested that during the non-number plate task, subjects allocated more attention and memory processing than for the number plate task [70]. Elevated P300 amplitudes were found for increased attention [71], and they indicate increased consciousness [72] with the quality of selection [73]. Reduced amplitudes and longer latencies and processing times were found during periods of lower attention [74, 75]. In this study, non-number plate stimuli evoked higher amplitudes and longer latencies of the P300 ERP component at most electrode sites This result suggests that subjects paid more voluntary attention to quality selection, which took more information processing time for non-number plate stimuli compared with number stimuli.

Concerning the neural sources of P300, based on the result of the scalp topographic map, interestingly, the distribution of magnitudes for the non-number plate was greater in the right hemisphere, whereas, conversely for the number plate, it was greater in the left hemisphere, indicating a left/right asymmetry of a neural response pattern for these two stimuli in the brain. Additionally, based on the results of cortical activation patterns, remarkably, some brain areas are activated both during number and non-number plate tasks, such as the bilateral inferior parietal lobule and temporal lobe. Strikingly, the frontal lobe activation especially in the left inferior frontal gyrus (Broca's area) was found only during the number plate task. Number recognition was not only a process of visual perception

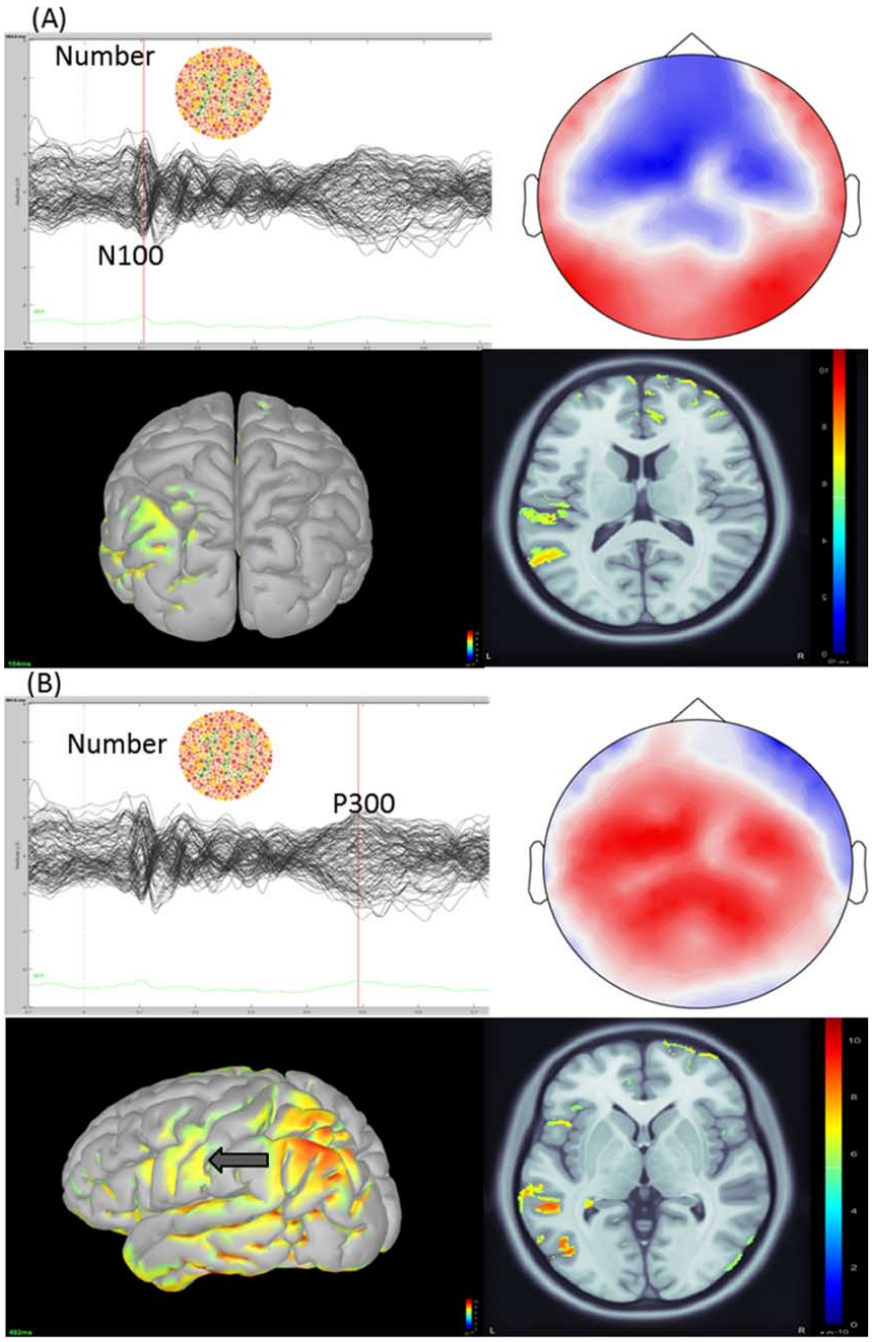

Fig. 4. EEG waveform, scalp topography, and cortical activations during number plate task. Upper left panel of figure (A), EEG time series of all 128 channels, *y*-axis and *x*-axis give amplitude (μV) & time (ms), respectively, white and red dotted lines indicate stimulation start time marked at 0 ms peak N100 ERP response (104 ms), respectively. Upper right panel gives scalp topographic map plotted from N100 peak. Lower panel of figure (A), cortical activations of N100 peak response are displayed as MRI 3D view with color bar (left side) and as axial MRI view with color bar (right side). Lower left panel of figure (B), EEG time series of 128 channels, *y*-axis and *x*-axis gives amplitude (μV) & time (ms), respectively. White dotted line gives stimulation start time (0 ms) and red line denotes peak P300 ERP response (492 ms), upper right panel shows scalp topographic map plotted from P300 peak. Lower panel of figure (A), cortical activations of P300 peak response are displayed on MRI 3D view with color bar (left side) and with axial MRI viewer, color bar (right side).

and attention, but was also related to the higher level of the cognitive function of language. This propensity was further supported by the effective connectivity analysis undertaken for this study, as it was in a previous study of blind people [76]. Neural correlates and functional measurement of number representations are complex occurrences when their semantic category is assimilated with shape and color categories. Number recognition, which can be associated with numerosity and the identification of the inherent magnitude of a number, can be a visual number shape (e.g. Arabic digit) that is culturally learned through education after birth. Activation of bilateral occipitotemporal cortex associated with the shape coding of non-numbers as opposed to numbers, was found in this study.

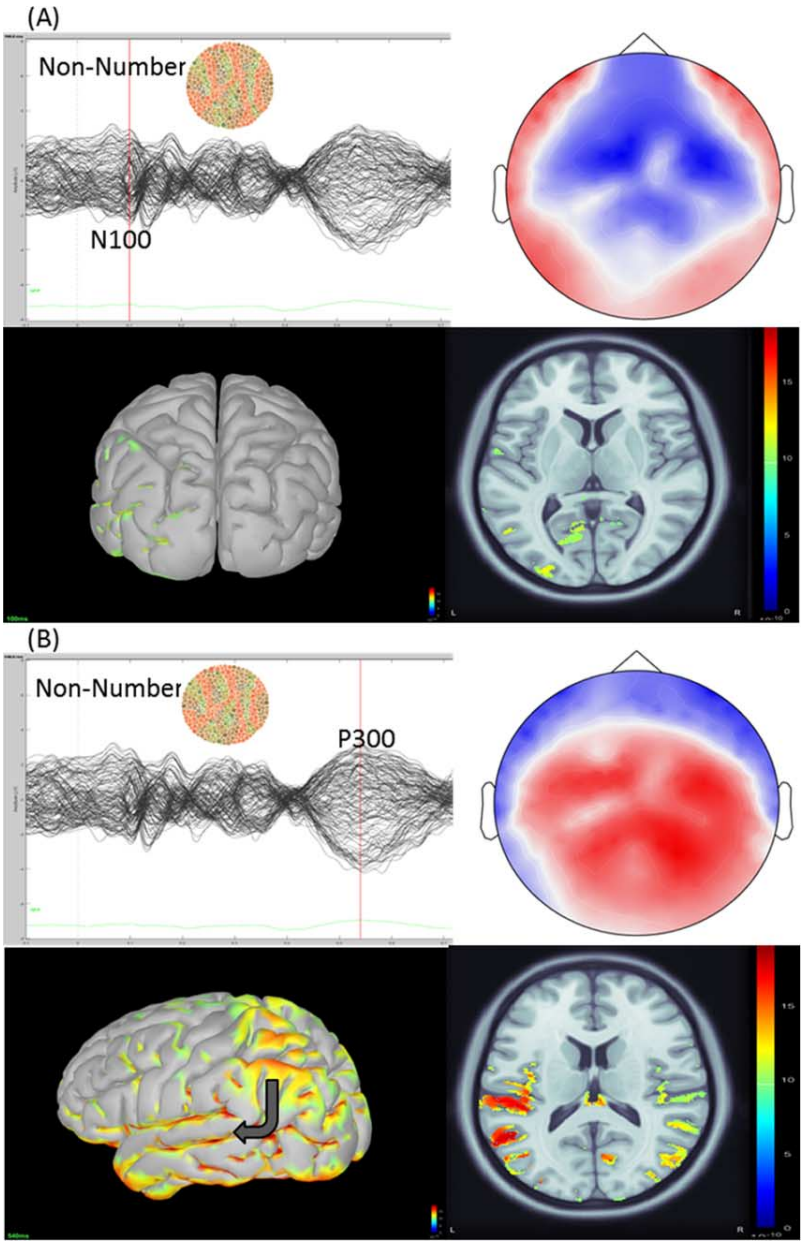

Fig. 5. EEG waveform, scalp topography, and cortical activations during non-number plate task. Upper left panel (A), EEG time series of all 128 channels, *y*-axis and *x*-axis give amplitude (μV) & time (ms) respectively, white dotted line gives stimulation start time (0 ms) and red line gives peak N100 ERP response (100 ms), upper right panel shows scalp topographic map plot at N100 peak. Lower panel (A), cortical activations of N100 peak response are displayed as MRI 3D view with color bar (left side) and as axial MRI view with color bar (right side). Lower left panel (B), EEG time series of 128 channels, *y*-axis and *x*-axis give amplitude (μV) & time (ms), respectively, white dotted line gives stimulation start time (0 ms) and red line indicates peak P300 ERP response (540 ms), upper right panel gives scalp topographic map plotted at P300 peak. Lower panel (A), cortical activations of P300 peak response are given as MRI 3D view with color bar (left side) and as an axial MRI view with color bar (right side).

Conversely, bilateral occipitotemporal activation based on the shape coding of Arabic digits and other numeric symbols was found in a study of macaque monkey brain that investigated neurophysiological evidence for a neural code for numbers [77]. However, in the current study, the right inferior temporal cortex activation during number plate tasks was consistent with findings reported by others [78, 79]. Additionally, during number plate tasks, the language area (LBA45) was activated, which is a similar result to that reported for a study of Arabic number reading [80]. Nonetheless, language area activation did not occur during non-number tasks in this study. Taken together, however, visual recognition of numbers dissociates from the recognition of non-numbers for both behavioral data and at the neural level, as similarly found in a study of neural double dissociation between letter and number recognition [81].

Granger causality analysis has received much attention in the study of language processing and the interactions of brain areas in large neural networks [82]. Throughout connectivity analysis, results reported here for effective connectivity revealed that there

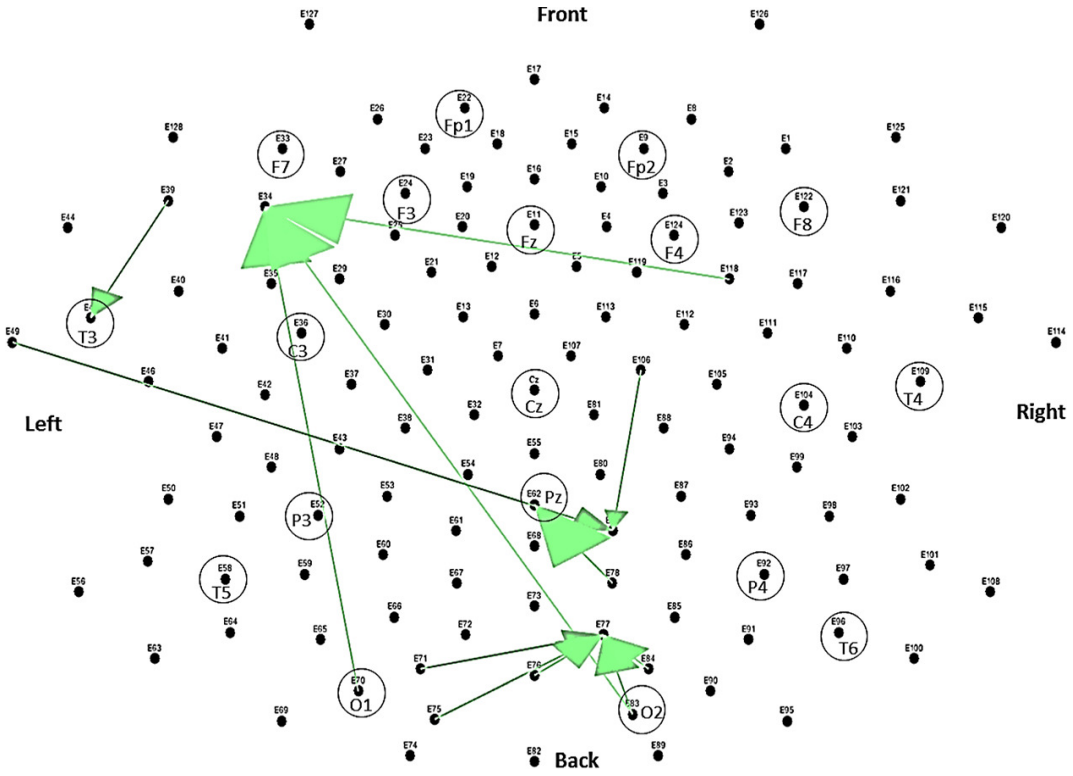

Fig. 6. Effective connectivity visualization from grand averaged wave form during presentation of number plates of an Ishihara color vision test from all recorded 128 channels of EGI system, circle indicates 19 electrode sites in 10–20 international system.

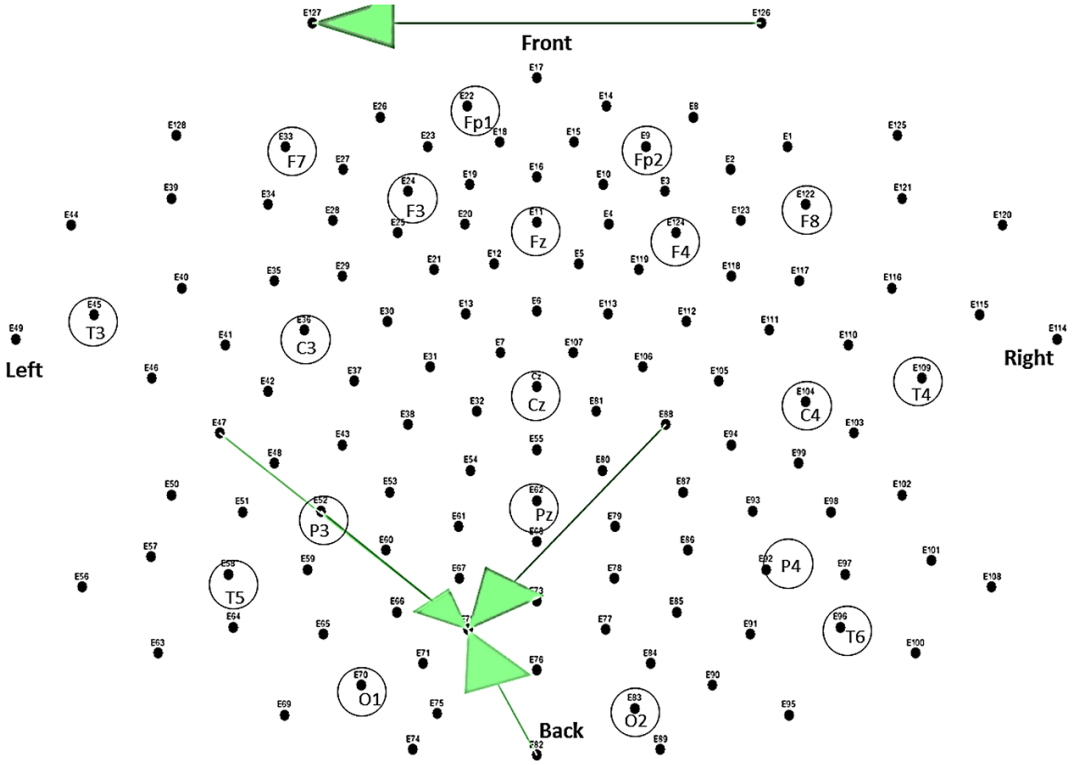

Fig. 7. Effective connectivity visualization from grand averaged waveform during presentation of non-number plates of an Ishihara color vision test from all recorded 128 channels of EGI system, circle indicates 19 electrode sites in 10–20 international system.

was clearly a strong interaction between occipital (O1 & O2) and left lateral frontal cortices (near the F7 electrode) during number plate tasks. The direction of coupling was from a visual occipital area towards a language area associated with semantic coding during number recognition, thus showing a stimulus-driven bottom-up effect in the defined neural networks. However, this effect was restricted to the occipital area during the non-number task.

5. Conclusion

In summary, to assess attention during numerical information processing, the visual cognitive function of ERP waveforms was investigated by use of Ishihara pseudoisochromatic plates. Results suggest that the visual identification of the two different stimuli were almost identical. However, the number information was processed spontaneously and was faster than the processing of non-number information. Attention load was relatively higher and delayed in the decision-making process of the non-number task. More interestingly, distribution of the source of attention control and the effects of attention on information processing were different for number and non-number tasks. Finally, this study is the first to report the use of easily administrable and readily available pseudoisochromatic plates to evaluate visual numerical cognition. These plates could provide an important tool to test attention deficit and connectivity disorders in anatomically and physiologically distinct brain networks.

Acknowledgments

This work was supported by a short term grant of Universiti Sains Malaysia (USM) (304/PPSP/ 61311092) for the author T.B.

Conflict of Interest

All authors declare no conflicts of interest.

References

[1] DeYoe EA, Van Essen DC (1988) Concurrent processing streams in monkey visual cortex. *Trends in Neurosciences* **11(5)**, 219-226.

[2] Köhler S, Kapur S, Moscovitch M, Winocur G, Houle S (1995) Dissociation of pathways for object and spatial vision: a PET study in humans. *Neuroreport: an International Journal for the Rapid Communication of Research in Neuroscience* **6(14)**, 1865-1868

[3] Chang S, Pearson J (2017) The functional effects of prior motion imagery and motion perception. *Cortex: a Journal Devoted to the Study of the Nervous System and Behavior* **105**, 83-96

[4] Roldan SM (2017) Object recognition in mental representations: Directions for exploring diagnostic features through visual mental imagery. *Frontiers in Psychology* **8**, 833.

[5] Sharpe LT, Stockman A, Jägle H, Nathans J (1999) Opsin genes, cone photopigments, color vision, and color blindness. *Color vision: From Genes to Perception*, 3-51.

[6] Smith VC, Pokorny J (1996) The design and use of a cone chromaticity space: a tutorial. *Color Research & Application* **21(5)**, 375-383.

[7] Belcher S, Greenshields K, Wright W (1958) Colour vision survey: using the Ishihara, Dvorine, Boström and Kugelberg, Boström, and American-Optical Hardy-Rand-Rittler tests. *The British Journal of Ophthalmology* **42(6)**, 355.

[8] Dain SJ (2004) Clinical colour vision tests. *Clinical and Experimental Optometry* **87(4, 5)**, 276-293.

[9] Arend LE, Reeves A, Schirillo J, Goldstein R (1991) Simultaneous color constancy: papers with diverse Munsell values. *Journal of the Optical Society of America* **8(4)**, 661-672.

[10] Fairchild MD (2013) *Color appearance models*. West Sussex, John Wiley & Sons.

[11] Goodale MA, Milner AD (1992) Separate visual pathways for perception and action. *Trends in Neurosciences* **15(1)**, 20-25.

[12] Mishkin M, Ungerleider LG, Macko KA (1983) Object vision and spatial vision: two cortical pathways. *Trends in Neurosciences* **6**, 414-417.

[13] Knops A (2017) Probing the neural correlates of number processing. *The Neuroscientist* **23(3)**, 264-274.

[14] Connaughton VM, Amiruddin A, Clunies-Ross KL, French N, Fox AM (2017) Assessing hemispheric specialization for processing arithmetic skills in adults: A functional transcranial doppler ultrasonography (fTCD) study. *Journal of Neuroscience Methods* **283**, 33-41.

[15] Dehaene S (1992) Varieties of numerical abilities. *Cognition* **44(1, 2)**, 1-42.

[16] Neisser U (1977) Cognitive psychology. *Science* **198**, 816-817.

[17] Barsalou LW (2014) *Cognitive psychology: An overview for cognitive scientists*. Hillsdale, NJ, US, Lawrence Erlbaum Associates.

[18] De Raad, B (2006) Individuality and Personality, Psychological Concepts: An International Historical Perspective. In, Pawlik K and d'Ydewalle G(Eds.)*Psychological Concepts: An International Historical Perspective*(pp. 299-323).East Sussex, UK, Psychology Press.

[19] MS M (1997) Cognition and Reality by Ulric Neisser. *The American Journal of Psychology* **90(3)**, 541-543.

[20] Miller EK, Cohen JD (2001) An integrative theory of prefrontal cortex function. *Annual Review of Neuroscience* **24(1)**, 167-202.

[21] Yeo DJ, Wilkey ED, Price GR (2017) The search for the number form area: A functional neuroimaging meta-analysis. *Neuroscience & Biobehavioral Reviews* **78**, 145-160.

[22] Sporns O, Honey CJ, Kötter R (2007) Identification and classification of hubs in brain networks. *Plos One* **2(10)**, e1049.

[23] Esposito F, Bertolino A, Scarabino T, Latorre V, Blasi G, Popolizio T, Tedeschi G, Cirillo S, Goebel R, Di Salle F (2006) Independent component model of the default-mode brain function: Assessing the impact of active thinking. *Brain Research Bulletin* **70(4-6)**, 263-269.

[24] Horovitz SG, Fukunaga M, de Zwart JA, van Gelderen P, Fulton SC, Balkin TJ, Duyn JH (2008) Low frequency BOLD fluctuations during resting wakefulness and light sleep: A simultaneous EEG-fMRI study. *Human Brain Mapping* **29(6)**, 671-682.

[25] Bassett DS, Wymbs NF, Porter MA, Mucha PJ, Carlson JM, Grafton ST (2011) Dynamic reconfiguration of human brain networks during learning. *Proceedings of the National Academy of Sciences* **108(18)**, 7641-7646.

[26] Hutchison RM, Womelsdorf T, Allen EA, Bandettini PA, Calhoun VD, Corbetta M, Della Penna S, Duyn JH, Glover GH, Gonzalez-Castillo J (2013) Dynamic functional connectivity: promise, issues, and interpretations. *Neuroimage* **80**, 360-378.

[27] Dosenbach NU, Fair DA, Cohen AL, Schlaggar BL, Petersen SE (2008) A dual-networks architecture of top-down control. *Trends in Cognitive Sciences* **12(3)**, 99-105.

[28] Koyama MS, Di Martino A, Kelly C, Jutagir DR, Sunshine J, Schwartz SJ, Castellanos FX, Milham MP (2013) Cortical signatures of dyslexia and remediation: an intrinsic functional connectivity approach. *Plos One* **8(2)**, e55454.

[29] Ghuntla TP, Mehta HB, Gokhale PA, Shah CJ (2014) Influence of practice on visual reaction time. *Journal of Mahatma Gandhi Institute of Medical Sciences* **19(2)**, 119.

[30] Horowitz-Kraus T, DiFrancesco M, Kay B, Wang Y, Holland SK (2015) Increased resting-state functional connectivity of visual-and cognitive-control brain networks after training in children with reading difficulties. *NeuroImage: Clinical* **8**, 619-630.

[31] Liu J, Zhang H, Chen C, Chen H, Cui J, Zhou X (2017) The neural circuits for arithmetic principles. *NeuroImage* **147**, 432-446.

[32] Galton F (1880) Visualised Numerals. *Nature* **21**, 494-495.

[33] Ramachandran VS, Hubbard EM (2001) Psychophysical investigations into the neural basis of synaesthesia. *Proceedings of the Royal Society of London B: Biological Sciences* **268(1470)**, 979-983.

[34] Brang D, Hubbard EM, Coulson S, Huang M, Ramachandran VS (2010) Magnetoencephalography reveals early activation of V4 in grapheme-color synesthesia. *Neuroimage* **53(1)**, 268-274.

[35] Mattingley JB, Payne JM, Rich AN (2006) Attentional load attenuates synaesthetic priming effects in grapheme-colour synaesthesia. *Cortex* **42(2)**, 213-221.

[36] Moore T and Zirnsak M (2017) Neural Mechanisms of Selective Visual Attention. *Annual Review of Psychology* **68(1)**, 47-72.

[37] Posner MI, Nissen MJ, Ogden WC (1978) Attended and unattended processing modes: The role of set for spatial location. In, Modes of Perceiving and Processing Information, pp. 137-157.

[38] Baayen RH, Milin P (2010) Analyzing reaction times. *International Journal of Psychological Research* **3(2)**, 12-28.

[39] Laming DRJ (1968) *Information theory of choice-reaction times*. Oxford, England, Academic Press.

[40] Welford AT (1980) Choice reaction time: Basic concepts. In, AT. Welford (Eds.)*Reaction Times* (pp. 73-128). New York, Academic Press.

[41] Lit A, Young RH, Shaffer M (1971) Simple time reaction as a function of luminance for various wavelengths. *Perception & Psychophysics* **10(6)**, 397-399.

[42] Misra N, Mahajan K, Maini B (1885) Comparative study of visual and auditory reaction time of hands and feet in males and females. *Indian Journal of Physiol Pharmacol* **29(4)**, 213-218.

[43] Spirduso WW (1975) Reaction and movement time as a function of age and physical activity level. *Journal of Gerontology* **30(4)**, 435-440.

[44] Gavkare AM, Nanaware NL, Surdi AD (2013) Auditory reaction time, visual reaction time and whole body reaction time in athletes. *Indian Medical Gazette* **6**, 214-219.

[45] Rugani R, Betti S, Ceccarini F, Sartori L (2017) Act on numbers: numerical magnitude influences selection and kinematics of finger movement. *Frontiers in Psychology* **8**, 1481.

[46] Sur S, Sinha V (2009) Event-related potential: An overview. *Industrial Psychiatry Journal* **18(1)**, 70-73.

[47] Du Y, Zhang Q, Zhang JX (2014) Does N200 reflect semantic processing? — An ERP study on Chinese visual word recognition. *Plos One* **9(3)**, e90794.

[48] Rugg M, Milner A, Lines C, Phalp R (1987) Modulation of visual event-related potentials by spatial and non-spatial visual selective attention. *Neuropsychologia* **25(1)**, 85-96.

[49] Vogel AC, Petersen SE, Schlaggar BL (2014) The VWFA: it's not just for words anymore. *Frontiers in Human Neuroscience* **8**, 88.

[50] Delb W, Strauss DJ, Low YF, Seidler H, Rheinschmitt A, Wobrock T, D'Amelio R (2008) Alterations in Event Related Potentials (ERP) associated with tinnitus distress and attention. *Applied Psychophysiology and Biofeedback* **33(4)**, 211-221.

[51] van der Stelt O, Kok A, Smulders FT, Snel J, Gunning WB (1998) Cerebral event-related potentials associated with selective attention to color: developmental changes from childhood to adulthood. *Psychophysiology* **35(3)**, 227-239.

[52] Picton TW (1992) The P300 wave of the human event-related potential. *Journal of Clinical Neurophysiology* **9(4)**, 456-479.

[53] Polich J, Kok A (1995) Cognitive and biological determinants of P300: an integrative review. *Biological Psychology* **41(2)**, 103-146.

[54] Cavina-Pratesi C, Kentridge R, Heywood C, Milner A (2010) Separate channels for processing form, texture, and color: evidence from fMRI adaptation and visual object agnosia. *Cerebral Cortex* **20(10)**, 2319-2332.

[55] Hasan RA, Reza F, Begum T. (2016) Education Level is associated with specific N200 and P300 profiles reflecting higher cognitive functioning. *Journal of Advances in Medical and Pharmaceutical Sciences* **10(4)**, 1-12.

[56] Fonteneau E, Davidoff J (2007) Neural correlates of colour categories. *Neuroreport* **18(13)**, 1323-1327.

[57] Tadel F, Baillet S, Mosher JC, Pantazis D, Leahy RM (2011) Brainstorm: a user-friendly application for MEG/EEG analysis. *Computational Intelligence and Neuroscience* **2011**, 879716.

[58] Niso G, Bruña R, Pereda E, Gutiérrez R, Bajo R, Maestú F, del-Pozo F (2013) HERMES: towards an integrated toolbox to characterize functional and effective brain connectivity. *Neuroinformatics* **11(4)**, 405-434.

[59] Miyahara E (2008) Errors reading the Ishihara pseudoisochromatic plates made by observers with normal colour vision. *Clinical and Experimental Optometry* **91(2)**, 161-165.

[60] Cosstick M, Robaei D, Rose K, Rochtchina E, Mitchell P (2005) Numerical confusion errors in ishihara testing: findings from a population-based study. *American Journal of Ophthalmology* **140(1)**, 154-156.

[61] Luck S (2005) *An introduction to the event-related potential technique*. Massachusetts, The MIT Press.

[62] Van Overwalle F, Van den Eede S, Baetens K, Vandekerckhove M (2009) Trait inferences in goal-directed behavior: ERP timing and localization under spontaneous and intentional processing. *Social Cognitive and Affective Neuroscience* **4(2)**, 177-190.

[63] Spence C, Parise C (2010) Prior-entry: A review. *Consciousness and Cognition* **19(1)**, 364-379.

[64] Hopf J-M, Vogel E, Woodman G, Heinze HJ, Luck SJ (2002) Localizing visual discrimination processes in time and space. *Journal of Neurophysiology* **88(4)**, 2088-2095.

[65] Eimer M (2014) The time course of spatial attention: insights from event-related brain potentials. *The Oxford Handbook of Attention* **1**, 289-317.

[66] Chayer C, Freedman M (2001) Frontal lobe functions. *Current Neurology and Neuroscience Reports* **1(6)**, 547-552.

[67] Hansenne M (2000) The p300 cognitive event-related potential. I. Theoretical and psychobiologic perspectives. *Clinical Neurophysiology* **30(4)**, 191-210.

[68] Patrick CJ, Bernat EM, Malone SM, Iacono WG, Krueger RF, McGue M (2006) P300 amplitude as an indicator of externalizing in adolescent males. *Psychophysiology* **43(1)**, 84-92.

[69] Polich J (1999), P300 in clinical applications. In: E. Niedermeyer and F. Lopes da Silva, (eds) *Electroencephalography: Basic Principles, Clinical Applications and Related Fields*(pp. 1073-1091), 4th edn. Urban & Schwarzenberg, Baltimore.

[70] Dehaene S, Kerszberg M, Changeux JP (1998) A neuronal model of a global workspace in effortful cognitive tasks. *Proceedings of the National Academy of Sciences* **95(24)**, 14529-14534.

[71] Russo PM, De Pascalis V, Varriale V, Barratt ES (2008) Impulsivity, intelligence and P300 wave: an empirical study. *International Journal of Psychophysiology* **69(2)**, 112-118.

[72] Dehaene S, Kerszberg M, Changeux JP (1998) A neuronal model of a global workspace in effortful cognitive tasks. *Proceedings of the National Academy of Sciences of the United States of America* **95**, 14529–14534.

[73] Jonkman L, Kemner C, Verbaten M, Van Engeland H, Camfferman G, Buitelaar J, Koelega H (2000) Attentional capacity, a probe ERP study: differences between children with attention-deficit hyperactivity disorder and normal control children and effects of methylphenidate. *Psychophysiology* **37(3)**, 334-346.

[74] Kleih S, Nijboer F, Halder S, Kübler A (2010) Motivation modulates the P300 amplitude during brain–computer interface use. *Clinical Neurophysiology* **121(7)**, 1023-1031.

[75] Brookhuis KA, Mulder G, Mulder L, Gloerich A (1983) The P3 complex as an index of information processing: The effects of response probability. *Biological Psychology* **17(4)**, 277-296.

[76] Abboud S, Maidenbaum S, Dehaene S, Amedi A (2015) A number-form area in the blind. *Nature Communications* **6**, 6026.

[77] Piazza M, Eger E (2016) Neural foundations and functional specificity of number representations. *Neuropsychologia* **83**, 257-273.

[78] Shum J, Hermes D, Foster BL, Dastjerdi M, Rangarajan V, Winawer J, Miller KJ, Parvizi J (2013) A brain area for visual numerals. *Journal of Neuroscience* **33(16)**, 6709-6715.

[79] Grotheer M, Herrmann KH, Kovács G (2016) Neuroimaging evidence of a bilateral representation for visually presented numbers. *Journal of Neuroscience* **36(1)**, 88-97.

[80] Roux FE, Lubrano V, Lauwers-Cances V, Giussani C, Démonet JF (2008) Cortical areas involved in Arabic number reading. *Neurology* **70(3)**, 210-217.

[81] Park J, Hebrank A, Polk TA, Park DC (2012) Neural dissociation of number from letter recognition and its relationship to parietal numerical processing. *Journal of Cognitive Neuroscience* **24(1)**, 39-50.

[82] Gow Jr DW, Caplan DN (2012) New levels of language processing complexity and organization revealed by granger causation. *Frontiers in Psychology* **19(3)**, 506.